Highly enantiodifferentiating site of human serum albumin for meditating photocyclodimerization of 2-anthracenecarboxylate elucidated by site-specific inhibition/quenching with xenon

Masaki Nishijima, Tamara C. S. Pace, Cornelia Bohne, Tadashi Mori, Yoshihisa Inoue & Takehiko Wada

December 2015

https://doi.org/10.1016/j.jphotochem.2015.12.019

Highly enantiodifferentiating site of human serum albumin for mediating photocyclodimerization of 2-anthracenecarboxylate elucidated by site-specific inhibition/quenching with xenon

Masaki Nishijima[a,*], Tamara C. S. Pace[b], Cornelia Bohne[b], Tadashi Mori[c], Yoshihisa Inoue[c], Takehiko Wada[d]

[a] *Office for University-Industry Collaboration, Osaka University, 2-8 Yamada-oka, Suita 565-0871, Japan*

[b] *Department of Chemistry, University of Victoria, P.O. Box 3065, Victoria, British Columbia V8W 3V6, Canada*

[c] *Department of Applied Chemistry, Osaka University, 2-1 Yamada-oka, Suita 565-0871, Japan*

[d] *Institute of Multidisciplinary Research for Advanced Materials, Tohoku University, 2-1-1 Katahira, Aoba-ku, Sendai 980-8577, Japan*

This paper is dedicated to Professor Yoshihisa Inoue on the occasion of his retirement from Osaka University.

* Corresponding author. Tel.: +81 6 6879 4206; fax: +81 6 6879 4208.
E-mail address: nishijima@uic.osaka-u.ac.jp (M. Nishijima).

Abstract

Complementary to the previous assignment of the first, second, and fourth binding sites of human serum albumin (HSA) for 2-anthracenecarboxylate (AC) and the subsequent mediation of AC photocyclodimerization, the site-specific inhibition of the enantiodifferentiation by xenon allowed us to assign the remaining third and fifth AC-binding sites to subdomains IB and IIIB, respectively. This study reveals a clearer picture of the binding and photochirogenic behavior of HSA and further expands the scope of bio-supramolecular photochirogenesis.

Keywords: Photochirogenesis; 2-Anthracenecarboxylate; Photocyclodimerization; Human serum albumin; Xenon

1. Introduction

Supramolecular photochirogenesis with biomolecular hosts [1], such as cyclic oligosaccharides [2], double stranded DNA [3], and transport proteins [4-7], enables us to both exploit the three-dimensionally well-defined hydrophobic cavity, groove, or pocket of the host as an inherently chiral environment for differentiating the enantio- or diastereotopic faces of a prochiral substrate upon supramolecular complexation in the ground state and execute supramolecular-to-molecular chirality transfer in the excited state. Among the bio-supramolecular hosts employed for photochirogenesis, human serum albumin (HSA) has particular advantages (and some complexities)

owing to its wide guest diversity, ample site information, and well-established binding properties for a range of endo- and exogenous ligands [8]. Exploiting these advantages, Zandomeneghi *et al.* achieved the photochemical kinetic resolution of racemic 1,1′-binaphthol with HSA [4], and Miranda *et al.* revealed the photophysical behavior of various aromatic compounds bound to HSA using laser flash photolysis [6]. More recently, Yokoyama *et al.* reported the enantioselective photochromic conversion of prochiral diarylethenes in HSA [7]. Moreover, we have achieved the highly enantiodifferentiating photocyclodimerization of 2-anthracenecarboxylate (AC) to stereoisomeric cyclodimers **1**–**4** mediated by HSA (Scheme 1), in which chiral cyclodimers **2** and **3** are formed in 80–90% enantiomeric excess (ee) upon irradiation of AC in the presence of HSA at an AC/HSA ratio of 3 [5]. The absolute configurations of the major enantiomers obtained for chiral **2** and **3** have been unambiguously determined as the (*M*)-enantiomers (Scheme 1) by comparing the experimental circular dichroism spectra with the theoretical ones calculated at the RI-CC2/TZVPP level [9].

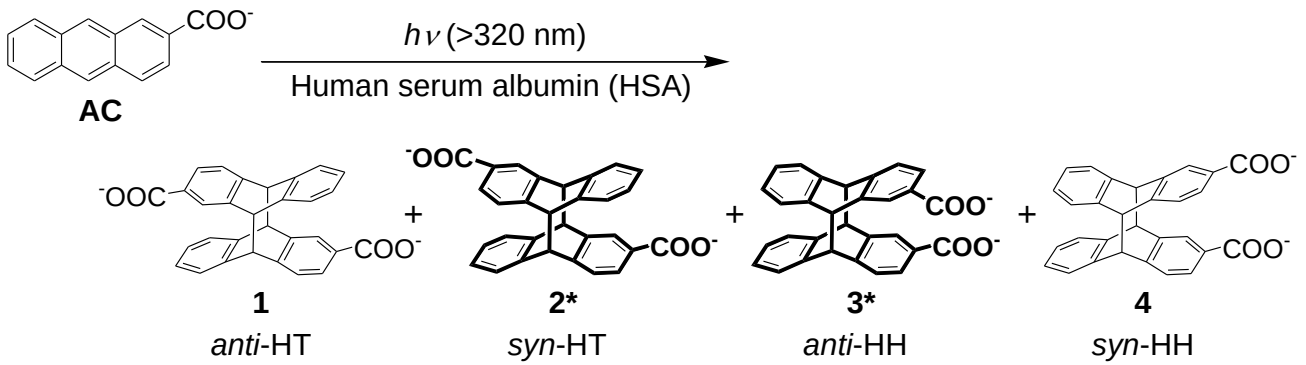

Scheme 1. Enantiodifferentiating photocyclodimerization of 2-anthracenecarboxylate (AC) mediated by human serum albumin (HSA). As illustrated, $\mathbf{2}_M$ and $\mathbf{3}_M$ are obtained as the major enantiomers [5b-d,9].

In a series of studies using site-specific drugs as binding inhibitors [5b-d], we have assigned the first (strongest) binding site for AC (with an association constant of 3×10^8 M^{-1}) in HSA to Sudlow Site 2 in subdomain IIIA, the second AC-binding site to Sudlow Site 1 in subdomain IIA, and the fourth AC-binding site to the sixth fatty acid site (FA6) in subdomain IIA-IIB. However, none of the site-specific binders examined appreciably altered the binding of AC to the third binding site or deteriorated the high enantioselectivity attained in this site. Thus, elucidation of the location of the highly enantiodifferentiating third site in HSA has been hindered. Intriguingly, a recent computational docking simulation study demonstrated that noble gases are bound to the fifth fatty acid site (FA5) located in subdomain IIIB of HSA with varying affinities in the order: He < Ne < Ar < Kr < Xe [10]. Xenon binding is of particular interest for bio-supramolecular photochirogenesis, as the bulky heavy atom not only occupies the FA5 site as a site-specific inhibitor, but also functions as a quencher of excited AC through spin-orbit coupling [11]. Indeed, a modest quenching rate constant (k_q) is reported for quenching of unsubstituted anthracene by xenon: $k_q = 6.9 \times 10^8$ M^{-1} s^{-1} in ethanol (approximately one order of magnitude smaller than the diffusion rate constant) [11c]. In the present study, we elucidated all five AC-binding sites distributed over the HSA subdomains by closely examining the effects of xenon on the product distribution and ee obtained for HSA-mediated photocyclodimerization of AC at varying AC/HSA ratios.

2. Experimental

2.1 Materials and instruments

Human serum albumin (fatty acid- and globulin-free grade, Sigma-Aldrich), 2-anthracenecarboxylic acid (Tokyo Chemical Industry), and xenon and argon gases (>99.995% purity, Air Liquide Japan or Airgas) were used as received. Other chemicals, solvents, and salts were purchased from Wako Pure Chemical Industries or Sigma-Aldrich.

UV-vis spectral changes of sample solutions containing AC and HSA upon photoirradiation were recorded on a JASCO UV-560 spectrophotometer. Chiral HPLC analyses were performed on a JASCO system equipped with a fluorescence detector (excitation at 254 nm and monitoring at 420 nm) [12] and tandem Cosmosil 5C18-AR-II (Nacalai Tesque) and Chiralcel OJ-RH (Daicel) columns operated at 35 °C. The samples were eluted with a 36:64 (v/v) mixture of acetonitrile and distilled water containing 0.1% trifluoroacetic acid at a flow rate of 0.5 mL min^{-1}. Steady-state fluorescence spectra were obtained using a JASCO FP-6500 or a PTI QM-2 fluorimeter. Time-resolved fluorescence measurements were carried out using an Edinburgh Instruments OB920 single photon counting system with a hydrogen flash lamp excitation source. The excitation and monitoring wavelengths were 394 and 420 nm, respectively. More detailed conditions were reported previously [5a-c].

2.2 Photoreaction and product analysis

All experiments were performed in 33 mM phosphate buffer at pH 7.0. A stock solution containing 5 mM AC was prepared by dissolving AC in a 10 mM aqueous NaOH solution. Sample solutions of different AC/HSA ratios (where the AC concentration was fixed at 60 μM) were prepared by diluting a given volume of the stock solution with freshly prepared aqueous buffer solutions of HSA at different concentrations. The sample solution (4 mL) thus prepared was placed in a conventional quartz cell with a septum cap, gently purged with argon or xenon gas for 10 min in an ice bath, and then irradiated at 25 °C in a temperature-controlled water bath with a 300-W high-pressure mercury lamp fitted with a uranium sleeve (effective wavelength: >320 nm). The irradiated solution was poured into an equal amount of acetonitrile with stirring, and the mixture was allowed to stand in the dark for at least 12 h. The resulting solution was ultrafiltrated with a membrane filter (Millipore Amicon Ultra, nominal molecular weight limit: >10 kDa), and the filtrate was subjected to chiral HPLC analysis.

2.3 Time-resolved experiments

For time-resolved experiments, the samples were prepared as described in Section 2.2 with a fixed AC concentration of 30 μM. The samples were bubbled with gases for at least 20 min. The number of counts collected in the channel with maximum intensity was 2,000, and the instrument response function (IRF) was determined by scattering light at the excitation wavelength using a Ludox solution. The decays were fit to a sum of exponentials (eq. 1), where τ_i corresponds to

individual lifetimes with corresponding pre-exponential factors A_i. The calculated decays were reconvoluted with the IRF and then compared to the experimental data. Fits were considered adequate when the residuals between the calculated and experimental data were random and the χ^2 value was between 0.9 and 1.2.

$$I(t) = I_0 \sum_1^i A_i e^{-t/\tau_i} \quad (1)$$

3. Results and discussion

3.1 Product studies

Photocyclodimerization of AC (60 μM) in the presence of native HSA at varying concentrations (6, 12, or 20 μM) was performed under an argon or xenon atmosphere in phosphate buffer at 25 °C. The photoreaction proceeded smoothly to afford cyclodimers **1**–**4** with the conversion, product distribution, and ee shown in Table 1. The product distribution is essentially equivalent to the product yield of each cyclodimer based on the conversion, as no side products are produced in appreciable yields.

Table 1

Enantiodifferentiating photocyclodimerization of 2-anthracenecarboxylate (AC) mediated by human serum albumin (HSA) under argon or xenon[a]

AC/ HSA	Atmosphere	Conversion[b] / %	Product distribution[c] / %				ee[d] / %		Yield based on AC used[e] / %					
			1	**2**	**3**	**4**	**2**	**3**	**1**	$\mathbf{2}_{M}$	$\mathbf{2}_{P}$	$\mathbf{3}_{M}$	$\mathbf{3}_{P}$	**4**
3	Ar	11	44	38	11	7	66	87	4.8	4.0	0.82	1.1	0.08	0.8
	Xe	10	46	41	9	4	65	89	4.6	3.7	0.79	0.9	0.05	0.4
5	Ar	41	44	42	9	5	71	42	18	15	2.6	2.6	1.1	2.1
	Xe	29	51	39	6	4	63	49	15	12	2.7	1.3	0.44	1.2
10	Ar	77	45	39	10	6	66	35	35	29	5.9	5.2	2.5	4.6
	Xe	57	52	36	7	5	57	0	30	23	6.3	2.0	2.0	3.1

[a] Aqueous buffer solutions (pH 7.0) of AC (60 μM) and HSA (6–20 μM) were irradiated at >320 nm for 1 h under argon or xenon at 25 °C. [b] Determined by monitoring the UV-vis spectral change of the 0-0 band of AC at 390 nm; error: <5%. [c] Essentially equal to the yield based on conversion (consumption of AC); error: <2%. [d] Enantiomeric excess determined by chiral HPLC; error: <5%; the positive ee values for **2** and **3** indicate the preferred formation of the (*M*)-enantiomers ($\mathbf{2}_{M}$ and $\mathbf{3}_{M}$). [e] Calculated from the conversion, product distribution, and enantiomer ratio (if applicable).

At the low AC/HSA ratio of 3, most AC molecules are bound to the non-productive first and second sites of HSA. The remaining AC populates the productive third site, where it relatively slowly photocyclodimerizes to **1**–**4**, affording **2** and **3** in high ee. Under this binding condition, xenon added to the system did not cause any significant changes (beyond the experimental errors) in conversion, product distribution, or ee, as shown in Table 1. The fact that the addition of xenon does not appreciably influence the photocyclodimerization behavior indicates that the third AC-binding site of HSA, where the majority of the photocyclodimerization takes place when AC/HSA = 3, is not in subdomain IIIB, which was demonstrated to stably accommodate xenon by the recent docking

simulation study [10].

When the AC/HSA ratio is increased to 5, the AC molecules populate mainly the first to third binding sites of HSA, which accommodate 1, 1, and 3 AC molecules, respectively [5b-d], while the equilibrium at the relatively weak third binding site allows partial population of the fourth and fifth sites. This means that the AC photocyclodimerization takes place not only in the third site, but also in the loosely binding fourth and fifth sites. Hence, the photoreaction is expected to proceed faster with different behavior of the product ee values, reflecting the enantioselectivities of these three independent AC-binding sites (third to fifth sites). Indeed, the conversion was greatly enhanced from 11% to 41% (note that the AC concentration was fixed at 60 μM and hence the number of absorbed photons was constant throughout the study) and the ee of **3** dramatically decreased from 87% at AC/HSA = 3 to 42% at AC/HSA = 5. In keen contrast, no apparent change was induced in the ee of **2** (71% at AC/HAS = 5 versus 66% at AC/HSA = 3). This result indicates that the photocyclodimerization in the fourth and fifth sites provides the same (*M*)-enantiomer of **2** (**2**$_{M}$) in an ee comparable to that obtained in the third site, but the formation of the antipodal (*P*)-enantiomer of **3** (**3**$_{P}$) partially cancels the high ee (87%) gained in the third site to afford the much lower ee of 42% [5b-d]. Intriguingly, the addition of xenon caused a decrease of the conversion from 41% to 29%, while the ee values of **2** and **3** were only slightly affected. A detailed analysis of the product yields based on AC conversion or the absolute amounts of the products (Table 1, right columns) revealed a global decrease of all the products, except **2**$_{P}$, suggesting less selective, nearly random inhibition

and/or quenching of excited AC in the fourth and/or fifth sites.

By further increasing the AC/HSA ratio to 10, the population of AC in the fourth and fifth sites is enhanced. As a consequence, the conversion further increased to 77%, while the ee of **2** remained at 66% and the ee for **3** decreased to 35%. In the presence of xenon, the conversion was significantly reduced to 57%, while the ee of **3** decreased dramatically to 0%. The formation of racemic **3** upon addition of xenon is rather unexpected, but can be rationalized by assuming that added xenon inhibited binding of AC to the fifth site and/or quenched AC bound to the fifth site. Accordingly, the amounts of $\mathbf{3}_{\boldsymbol{M}}$ produced in the third site and $\mathbf{3}_{\boldsymbol{P}}$ produced in the fourth site were balanced, resulting in the observed overall ee of 0%. This interpretation is compatible with our previous characterization of each binding site, which indicated that the third to fifth sites consistently afford $\mathbf{2}_{\boldsymbol{M}}$ in comparable ee, whereas antipodal $\mathbf{3}_{\boldsymbol{M}}$ and $\mathbf{3}_{\boldsymbol{P}}$ are produced in the third/fifth sites and fourth site, respectively [5d]. Thus, the xenon-inhibition/quenching experiment at AC/HSA = 10 allows us to assign the fifth binding site, in which the most effective inhibition/quenching occurred, to subdomain IIIB, which binds xenon [10].

As a transport protein, HSA possesses seven independent binding sites (most of which bind one or two fatty acid (FA) molecules) called FA*n* sites (*n* = 1–7, numbered in the order of affinity), which are distributed over subdomains IA (FA2), IB (FA1), IIA (FA7), IIA-IIB (FA6), IIIA (FA3,4), IIIB (FA5), and the cleft (which does not bind any FA molecules) [8]. In our previous study, we assigned the first, second, and fourth AC-binding sites to subdomains IIIA, IIA, and IIA-IIB, respectively [5d].

Using xenon as a site-specific inhibitor/quencher in the present study enabled us to allocate the fifth site to subdomain IIIB (FA5), leaving the highly enantiodifferentiating, Xe-insensitive third site unassigned. However, there remain only three candidates for the location of the third site: subdomains IA, IB, and the cleft. Of these, subdomain IA possesses a narrow pocket that binds the long alkyl chains of FA molecules [8c] and tetrahydrocannabinol [8d], but does not bind any bulky ligands, such as AC. In contrast, the cleft is a more hydrophilic site exposed to bulk water that allows ready penetration of outside xenon, which, if AC were bound to the cleft, would lead to dynamic quenching of excited AC. Consequently, it is likely that the third site is located in subdomain IB, which is known to bind large hydrophobic aromatic compounds, such as triiodobenzoate [8e], indomethacin [8e], and hemin [8f]. The interior walls of the binding pocket in subdomain IB are decorated with tyrosine (Y138 and Y161) and cationic amino acid residues (R114, R117, H146, and K190), which are suitable for π–π-stacking and electrostatic interactions with AC, and this binding pocket is also protected from outside xenon. These features are consistent with the complexation and photochirogenic behavior in the presence/absence of xenon observed in this study, allowing us to assign the highly enantiodifferentiating third AC-binding site to subdomain IB (FA1).

3.2 Photophysical studies

Although we could assign the highly enantiodifferentiating third site to subdomain IB from the product studies in the presence/absence of xenon, the exact role of xenon as a binding inhibitor

and/or an excited-state quencher is not very clear. To explore the function of xenon, we performed fluorescence quenching experiments and lifetime measurements for AC in the presence of HSA under argon and xenon, as summarized in Table 2.

Table 2

Relative steady-state fluorescence intensities (F/F_0) and fluorescence lifetimes (τ_i) with relative abundance (pre-exponential factor A_i) for aqueous buffer solutions of AC in the presence of HSA under argon or xenon[a]

AC/HSA	Atmosphere	F/F_0[b]	τ_1	A_1	τ_2	A_2	τ_3	A_3	χ^2
∞ (AC only)	Ar	-	16.4	1					1.062
	Xe	-	15.9 ± 0.1	1					1.070–1.092 (2)[d]
5	Ar	1	1.8[c]	0.42 ± 0.3	4.0[c]	0.2 ± 0.1	16.4 ± 0.1	0.38 ± 0.02	0.941–1.109 (2)
	Xe	0.95 ± 0.05	1.8[c]	0.42	4.0[c]	0.14	15.8	0.44	1.051
10	Ar	1	1.8[c]	0.15 ± 0.06	4.0[c]	0.11 ± 0.02	16.5 ± 0.2	0.73 ± 0.07	1.062–1.124 (3)
	Xe	1.00 ± 0.05	1.8[c]	0.1 ± 0.1	4.0[c]	0.2 ± 0.1	16.1 ± 0.1	0.73 ± 0.03	0.920–0.974 (2)

[a] [AC] = 30 μM (fixed) and [HSA] = 0, 3, or 6 μM in phosphate buffer (pH 7.0) at 25 °C. [b] Fluorescence intensity relative to the intensity under Ar at each AC/HSA ratio. [c] τ_1 and τ_2 were fixed to the values determined previously for AC bound to the first site of HSA (note that AC accommodated in the first site has two orientations that show distinctly different lifetimes) [5c,d], with the assumption that the added gas will have little effect on the short lifetimes of AC in this well-protected binding site. [d] Numbers in parentheses indicate the number of independent experiments for time-resolved studies. When no number is stated, the experiment was performed once.

The lifetime of AC in buffer solution in the presence of xenon was slightly shorter than that under argon (Table 2). The quenching rate constant (k_q) was estimated to be less than 4×10^8 M^{-1} s^{-1} using the equation $\tau_{Xe} = 1/(1/\tau_{Ar} + k_q[Xe])$, where τ_{Xe} and τ_{Ar} are the lifetimes of AC under xenon and argon, respectively, and [Xe] = 5 mM [13]. This value is in line with the rate constant observed in ethanol for quenching of the fluorescence of anthracene by xenon ($k_q = 6.9 \times 10^8$ M^{-1} s^{-1}) [11c].

In the presence of HSA, we observed three lifetimes of 1.8, 4.0, and ca. 16 ns, as reported previously [5b,c]. The first two lifetimes (τ_1 and τ_2) have been assigned to AC bound in different orientations to the hydrophobic first site. The third lifetime (τ_3) is the weight-averaged lifetime of AC molecules accommodated in the third, fourth, and/or fifth sites, which have very similar lifetimes to each other and also to that of AC in aqueous solution, reflecting the hydrophilic nature of these weaker binding sites [5b,c]. AC accommodated in the second site is fluorometrically silent due to efficient quenching by the tryptophan residue of HSA located at this site. At AC/HSA = 5, the addition of xenon only slightly reduced the τ_3 value, but no appreciable change was seen in the relative abundance (A_3). This result is reasonable as the population of AC in the Xe-binding fifth site is low at this AC/HSA ratio. The same result was observed when the AC/HSA ratio was increased to 10. In the presence of xenon, the majority of AC molecules are thought to populate the first to fourth sites, which formally can accommodate up to 10 AC molecules in total, and AC may also be displaced into water. The intensities of the steady-state spectra were normalized to the spectra for the solution purged with argon ($F/F_0 = 1$). The same intensities were observed for the spectra purged

with xenon, indicating that no static quenching occurred owing to incorporation of both AC and xenon in the same site. Therefore, the major role of xenon seems to be that it occupies the fifth AC-binding site of HSA, as no shortening of the excited state AC lifetimes was observed.

4. Conclusions

In this study, we employed xenon as a subdomain IIIB-specific inhibitor/quencher for the enantiodifferentiating photocyclodimerization of AC mediated by HSA. The detailed analyses of the photochirogenic behavior at various AC/HSA ratios in the presence/absence of xenon, as well as the site assignments reported previously [5b-d], enabled us to fully locate the five AC-binding sites of different photoreactivity and enantioselectivity that are populated over subdomains I–III of HSA. Figure 2 summarizes the binding site information for HSA revealed in the previous and present studies. The first, second, and fourth AC-binding sites have previously been assigned to Sudlow Site 2 (subdomain IIIA), Sudlow Site 1 (subdomain IIA), and subdomain IIA-IIB, respectively [5b-d]. In the present study, the fifth binding site was assignable to subdomain IIIB, which has high xenon affinity, because of the significantly reduced conversion and ee value observed upon addition of xenon at AC/HSA = 10. Among the remaining three binding sites available in HSA, the binding environments of subdomain IA and the cleft are too narrow for AC or incompatible with the photochirogenic behavior observed in the presence of xenon. The former site has only a tight space for accommodating a fatty acid, and the latter is exposed to bulk water, where bound AC would be

anticipated to suffer dynamic quenching by outside quenchers, such as nitromethane [5c] or xenon. Thus, subdomain IB is the most plausible third AC-binding site in view of its relatively wide interior space surrounded by aromatic and cationic amino acid residues capable of π–π-stacking and electrostatic interactions, which can accommodate anionic AC molecules in the binding pocket protected from interaction with outside xenon. The steady-state and time-resolved fluorescence studies suggest that xenon functions as a binding inhibitor, rather than as a quencher. The full assignment of the five AC-binding sites in HSA not only elucidates the binding and photochirogenic behavior of AC within HSA, but also enables us to expand the scope of bio-supramolecular photochirogenesis with HSA and the range of photosubstrates that can be employed. Furthermore, the methodologies developed in the previous and present studies should be widely applicable to other bio-supramolecular photochirogenic systems.

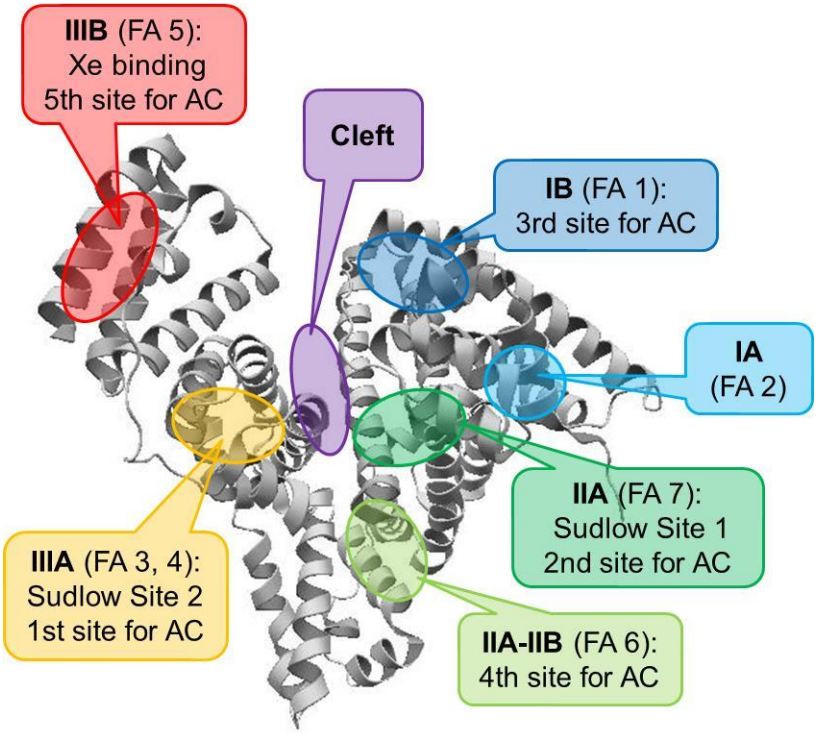

Figure 2. Summary of the binding sites located in subdomains IA (FA2), IB (FA1; AC3), IIA (FA7; AC2), IIA-IIB (FA6; AC4), IIIA (FA3,4; AC1), IIIB (FA5; AC4), and the cleft of HSA, where FA*n* and AC*n* refer to *n*th fatty acid and 2-anthracenecarboxylate sites, respectively.

Acknowledgments

This work was supported by Grant-in-Aids for Challenging Exploratory Research (No. 25620163) from the Japan Society for the Promotion of Science (JSPS), Network Joint Research Center for Advanced Materials and Devices, Shorai Foundation for Science and Technology, and Sumitomo Foundation, all of which are gratefully acknowledged. The authors at UVic thank the Natural Sciences and Engineering Research Council of Canada (NSERC) for funding.

References

[1] (a) Y. Inoue, V. Ramamurthy (Eds.), Chiral Photochemistry, Marcel Dekker, New York, 2004; (b) V. Ramamurthy, Y. Inoue (Eds.), Supramolecular Photochemistry, Wiley, Hoboken, NJ, 2011; (c) Z. Yan, W. Wu, C. Yang, Y. Inoue, Catalytic supramolecular photochirogenesis, Supramol. Catal. 2 (2015) 9–24; (d) V. Ramamurthy, B. Mondal, Supramolecular photochemistry concepts highlighted with select examples, J. Photochem. Photobiol. C 23 (2015) 68–102.

[2] C. Yang, Y. Inoue, Supramolecular photochirogenesis with cyclodextrin in: A. Douhal (Ed.), Cyclodextrin Materials Photochemistry, Photophysics and Photobiology, Elsevier, Amsterdam,

2006, pp. 241–266.

[3] T. Wada, N. Sugahara, M. Kawano, Y. Inoue, First asymmetric photochemistry with nucleosides and DNA: Enantiodifferentiating *Z–E* photoisomerization of cyclooctene, Chem. Lett. 10 (2000) 1174–1175.

[4] (a) N. Levi-Minzi, M. Zandomeneghi, Photochemistry in biological matrices: Activation of racemic mixtures and interconversion of enantiomers, J. Am. Chem. Soc. 114 (1992) 9300–9304; (b) C. Festa, N. Levi-Minzi, M. Zandomeneghi, Photochemistry in biological matrixes: Binding site photoreactivity of ketoprofen in serum albumins and chiral discrimination, Gazz. Chim. Ital. 126 (1996) 599–603; (c) A. Ouchi, G. Zandomeneghi, M. Zandomeneghi, Complexation with albumins of chiral aromatic substrates and their chemistry in ground and excited states. Catalytic and chirality recognition properties of the protein in the cases of binaphthol, its photoisomers, and ketoprofen, Chirality 14 (2002) 1–11; (d) M. Nishijima, J.-W. Chang, C. Yang, G. Fukuhara, T. Mori, Y. Inoue, Chiral recognition and supramolecular photoreaction of 1,1′-binaphthol with bovine and human serum albumins, Res. Chem. Intermed. 39 (2013) 371–383.

[5] (a) T. Wada, M. Nishijima, T. Fujisawa, N. Sugahara, T. Mori, A. Nakamura, Y. Inoue, Bovine serum albumin-mediated enantiodifferentiating photocyclodimerization of 2-anthracene-carboxylate, J. Am. Chem. Soc. 125 (2003) 7492–7493; (b) M. Nishijima, T. Wada, T. Mori, T.C.S. Pace, C. Bohne, Y. Inoue, Highly enantiomeric supramolecular [4 + 4] photocyclo-

dimerization of 2-anthracenecarboxylate mediated by human serum albumin, J. Am. Chem. Soc. 129 (2007) 3478–3479; (c) T.C.S. Pace, M. Nishijima, T. Wada, Y. Inoue, C. Bohne, Photophysical studies on the supramolecular photochirogenesis for the photocyclodimerization of 2-anthracenecarboxylate within human serum albumin, J. Phys. Chem. B 113 (2009) 10445–10453; (d) D. Fuentealba, H. Kato, M. Nishijima, G. Fukuhara, T. Mori, Y. Inoue, C. Bohne, Explaining the highly enantiomeric photocyclodimerization of 2-anthracenecarboxylate bound to human serum albumin using time-resolved anisotropy studies, J. Am. Chem. Soc. 135 (2013) 203–209; (e) M. Nishijima, H. Kato, G. Fukuhara, C. Yang, T. Mori, T. Maruyama, M. Otagiri, Y. Inoue, Photochirogenesis with mutant human serum albumins: Enantiodifferentiating photocyclodimerization of 2-anthracenecarboxylate, Chem. Commun. 49 (2013) 7433–7435; (f) M. Nishijima, H. Kato, C. Yang, G. Fukuhara, T. Mori, Y. Araki, T. Wada, Y. Inoue, Catalytic bio-supramolecular photochirogenesis: batch-operated enantiodifferentiating photocyclo-dimerization of 2-anthracenecarboxylate with human serum albumin, ChemCatChem 5 (2013) 3237–3240.

[6] (a) I. Vayá, C.J. Bueno, M.C. Jiménez, M.A. Miranda, Use of triplet excited states for the study of drug binding to human and bovine serum albumins, ChemMedChem 1 (2006) 1015–1020; (b) J. Rohacova, G. Sastre, L.M. Marin, M.A. Miranda, Dansyl labeling to modulate the relative affinity of bile acids for the binding sites of human serum albumin, J. Phys. Chem. B 115 (2011) 10518–10524; (c) M. Marin, V. Lhiaubet-Vallet, M.A. Miranda, Enhanced photochemical [6π]

electrocyclization within the lipophilic protein binding site, Org. Lett. 14 (2012) 1788–1791; (d) P. Bonancía, I. Vayá, M.C. Jiménez, M.A. Miranda, Intraprotein formation of a long wavelength absorbing complex and inhibition of excited-state deprotonation in a chiral hydroxybiphenyl, J. Phys. Chem. B 116 (2012) 14839–14843; (e) I. Vayá, V. Lhiaubet-Vallet, M.C. Jiménez, M.A. Miranda, Photoactive assemblies of organic compounds and biomolecules: Drug–protein supramolecular systems, Chem. Soc. Rev. 43 (2014) 4102–4122.

[7] M. Fukagawa, I. Kawamura, T. Ubukata, Y. Yokoyama, Enantioselective photochromism of diarylethenes in human serum albumin, Chem. Eur. J. 19 (2013) 9434–9437.

[8] (a) U. Kragh-Hansen, Molecular aspects of ligand binding to serum albumin, Pharmacol. Rev. 33 (1981) 17–53; (b) T. Peters Jr., All about Albumin: Biochemistry, Genetics, and Medical Applications, Academic Press, San Diego, 1996; (c) J. Ghuman, P.A. Zunszain, I. Petitpas, A.A. Battacharya, M. Otagiri, S. Curry, Structural basis of the drug-binding specificity of human serum albumin, J. Mol. Biol. 353 (2005) 38–52; (d) G. Fanali, Y. Cao, P. Ascenzi, V. Trezza, T. Rubino, D. Parolaro, M. Fasano, Binding of δ9-tetrahydrocannabinol and diazepam to human serum albumin, IUBMB Life 63 (2011) 446–451; (e) P.A. Zunszain, J. Ghuman, T. Komatsu, E. Tsuchida, S. Curry, Crystal structural analysis of human serum albumin complexed with hemin and fatty acid, BMC Struct. Biol. 3 (2003) 6; (f) P.A. Zunszain, J. Ghuman, A.F. McDonagh, S. Curry, Crystallographic analysis of human serum albumin complexed with 4*Z*,15*E*-bilirubin-IXα, J. Mol. Biol. 381 (2008) 394–406.

[9] A. Wakai, H. Fukasawa, C. Yang, T. Mori, Y. Inoue, Theoretical and experimental investigations of circular dichroism and absolute configuration determination of chiral anthracene photodimers, J. Am. Chem. Soc. 134 (2009) 4990–4997 and 10306 (erratum).

[10] T. Seto, H. Isogai, M. Ozaki, S. Nosaka, Noble gas binding to human serum albumin using docking simulation: nonimmobilizers and anesthetics bind to different sites, Anesth. Analg. 107 (2008) 1223–1228.

[11] (a) J.R. Lakowicz, Principle of Fluorescence Spectroscopy, third ed., Springer Publishing, New York, 2010; (b) A. Kearvell, F. Wilkinson, Fluorescence quenching and external spin-orbit coupling effects, Mol. Cryst. 4 (1968) 69–81; (c) A.R. Horrocks, A. Kearvell, K. Tickle, F. Wilkinson, Mechanism of fluorescence quenching in solution. Part 2.—Quenching by xenon and intersystem crossing efficiencies, Trans. Faraday Soc. 62 (1966) 3393–3399.

[12] M. Nishijima, T. Wada, K. Nagamori, Y. Inoue, High-sensitivity HPLC quantification of nonfluorescent but photolabile analyte through photoreversion in fluorescence detector, Chem. Lett. 38 (2009) 726–727.

[13] G.J. Ewing, L.G. Ionescu, Dissociation pressure and other thermodynamic properties of xenon-water clathrate, J. Chem. Eng. Data 19 (1974) 367–369.